Catalysis Letters
https://doi.org/10.1007/s10562-021-03719-0

Pd(II)-Metalated and L-Proline-Decorated Multivariate UiO-67 as Bifunctional Catalyst for Asymmetric Sequential Reactions

Lin Cheng[1] · Liumei Cao[1] · Hao Ren[1] · Qiaoqiao Guo[1] · Huifang Deng[1] · Yiming Li[1]

Received: 26 May 2021 / Accepted: 20 June 2021

Abstract

The construction of a multifunctional catalyst for multistep sequential\tandem reactions at the molecular level faces a formidable challenge. Multivariate (MTV)-MOFs can provide a facile and tunable platform for rationally designing such multifunctional catalysts via grafting different catalytic groups on the bridging ligands. However, the related investigations are still limited. Here, Pd(II) and L-proline are metalated and decorated to organic linkers, respectively, to build a MTV-MOF, which is then successfully applied to sequential Suzuki Coupling/asymmetric Aldol reactions with satisfied coupling performance (yields up to 99%) and good enantioselectivities (ee_{anti} up to 98%). Inductively coupled plasma optical emission spectrometer (ICP-OES) measurements of the supernatant and hot leaching test suggest the heterogeneous nature of the catalyst. Macrosubstrate tests verify that the reaction occurs inside the pores of the MOF. The heterogeneous catalyst can maintain structural stability and catalytic activity within three cycles.

Graphic Abstract

Versatile Pd(II) and L-proline were metalated and decorated, respectively, into stable UiO-67 to construct bifunctional and heterogeneous multivariate MOF catalyst, which displayed efficient and recyclable catalytic activity in sequential Suzuki Coupling/asymmetric Aldol reactions.

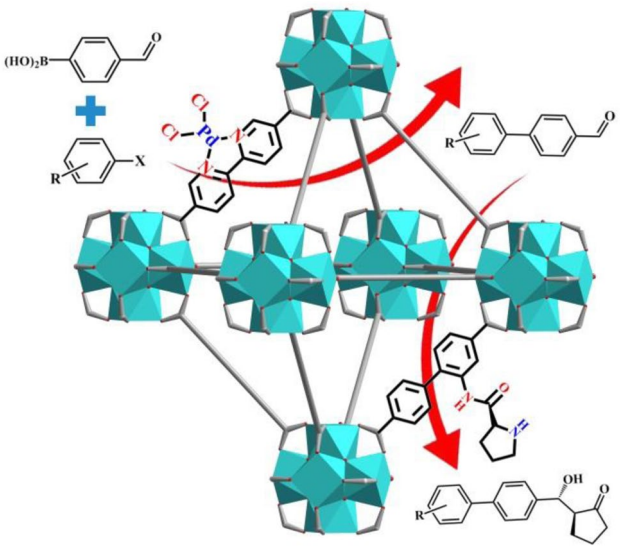

Keywords Chiral proline · UiO-67 · Heterogeneous catalyst · Bifunctional catalyst · Asymmetric sequential reactions

✉ Lin Cheng
lcheng@seu.edu.cn

[1] School of Chemistry and Chemical Engineering, Southeast University, Nanjing 210009, People's Republic of China

Published online: 28 June 2021

1 Introduction

Sequential reactions, combining multi-step organic synthetic procedures into one with a single catalyst, have aroused considerable interest because they can minimize chemical wastes, lower operation time, and avoid the isolation and purification of reaction intermediates [1, 2]. The single catalyst usually needs to own multifunctional active sites, achieving each step in sequence. However, the design and construction of such a multifunctional catalyst with two or more active sites at the molecular level is still a huge challenge owing to rapidly increased molecular complexity [3–5], high stability requirements of active sites under the reaction conditions of each catalytic step and the avoidance of the deactivation between incompatible active sites, such as acid–base [5–13]. Thus, looking for a universal strategy to unit different catalytic sites into a stable platform becomes particular important. Metal–organic frameworks (MOFs) can be regarded as an ideal and tunable platform for rationally designing heterogeneous multi-functional catalysts via precisely functionalizing metal nodes, organic linkers and encapsulated active species [14–23]. Compared with versatile and diverse organic ligands, the selection of open metal sites and encapsulated catalysts is always limited. Coordinately unsaturated metal sites are usually only used as Lewis acid catalysts [24–28], and immobilized species are often restricted to stable or large-size catalysts, such as metal and metal oxide nanoparticles, polymers, enzymes, etc., which are difficult to escape from the channels/holes of MOFs during the catalytic process [17]. For soluble or small molecules, such as metal salts and organic small molecules, which are widely applied as homogeneous catalysts in various reactions, it's hard to be introduced into MOFs as open metal sites or encapsulated catalysts. Fortunately, these organic small molecules can be easily decorated to the desired linkers of MOFs via multifarious organic synthetic methods [24–28], and metal ions can also be metalated into programmed coordinated sites of organic ligands [29–39]. Besides, the linkers can be easily modified via tailored chiral groups to construct chiral MOF catalysts and yet they have seldom been applied in asymmetric sequential/tandem reactions [40–48].

Multivariate (MTV)-MOFs, containing more than one organic linker with similar length, geometry and connectivity within a single framework, have been extensively investigated [49–74] since Yaghi and co-workers successfully introduced eight distinct functionalities in a single MOF via mixed-linker strategy [49]. The combination of two or more functional groups, grafted onto different bridging ligands, promotes MTV-MOFs to be reliable candidates for catalyzing multistep sequential reactions. Unfortunately, the investigation of multifunctional MTV-MOFs with mixed ligands on sequential/tandem catalysis has seldom reported [45–48, 69–74], and the rare examples were mainly focused on the cascade reactions catalyzed via mixed metallosalen linkers with different metal central sites [45–48].

Pd(II) salts, including $PdCl_2$ and $Pd(OAC)_2$, are a kind of famous catalysts for organic transformation. Because of their high price and limited resource, the full utilization of each Pd(II) catalytic site becomes a significant yet challenging task [9, 71]. The immobilization of isolated active single-site Pd(II) into the bipyridyl-containing ligands of MOFs via metalation interaction has offered a promising solution [9, 36, 75–77]. However, to our knowledge, Pd(II)-metalated MOFs have yet to be employed in asymmetric sequential/tandem reactions. Meanwhile, L-proline, a well-known privilege catalyst, has been successfully decorated to MOFs via coordination to open metal sites or grafting to organic linkers to construct chiral heterogeneous catalysts [44, 78–94].

Herein, UiO-67 with excellent chemical and thermal stability was selected as the parent MOF. $PdCl_2$ and L-proline were metalated and decorated, respectively, to UiO-67 via mixed-ligand strategy, resulting in a MTV-MOF (Scheme 1). The heterogeneous bifunctional catalyst was further applied in sequential Suzuki Coupling/asymmetric Aldol reactions, achieving satisfied coupling performance (yield up to 99%) and enantioselectivities (ee_{anti} up to 98%). To our knowledge, this was the first example of MTV-MOFs, dual-functionalized by metal salts and organic catalysts via mixed ligand strategy, which was applied in asymmetric sequential reactions.

2 Results and Discussion

2.1 Synthesis and Characterization of the Bifunctional Catalyst

Three organic ligands with similar length and coordination modes, were employed to construct the MTV-MOF, UiO-67-Pd-pro (Scheme 1), in which L-proline decorated ligand was fabricated via four-step process (Scheme S1), and Pd(II)-metalated ligand was synthesized by a bipyridine-based ligand, 2,2'-bipyridine-5,5'-dicarboxylic acid, with $PdCl_2$, via three-step synthesis (Scheme S2). UiO-67-Pd and UiO-67-pro, used in controlled experiments, were synthesized via the similar procedure to that of UiO-67-Pd-pro.

Powder X-ray diffraction (XRD) pattern of UiO-67-Pd-pro was identical to that of parent UiO-67 (Fig. 1), indicating that it was isostructural to UiO-67. ^{1}H-NMR spectroscopy of UiO-67-Pd-pro, after treated by dilute HF acidlysis, was performed to examine the ratio of three ligands. The ratio of L-proline decorated ligand,

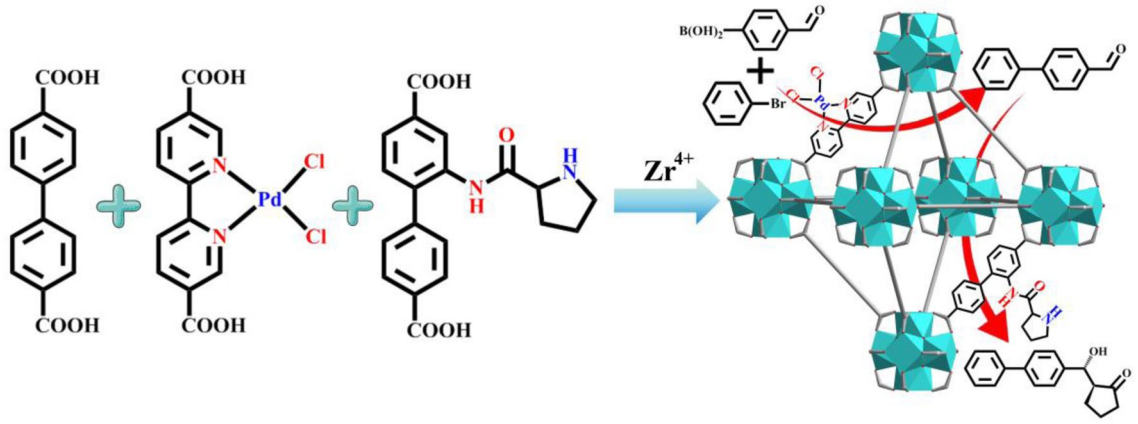

Scheme 1 Construction of multivariate UiO-67-Pd-pro via mixed-linker strategy and its application in sequential Suzuki Coupling/asymmetric Aldol reactions

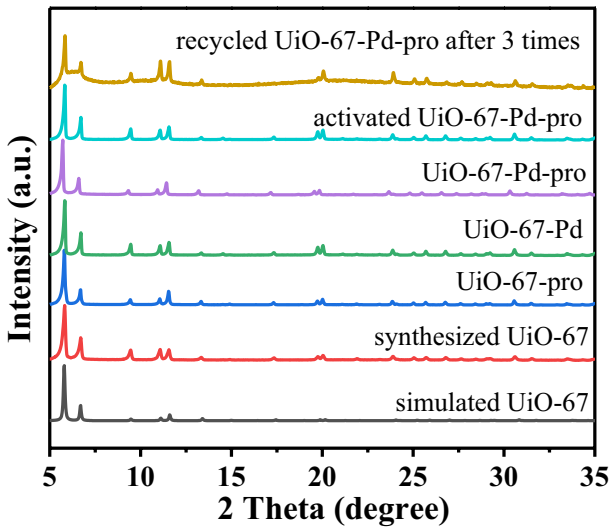

Fig. 1 PXRD patterns of the synthesized samples

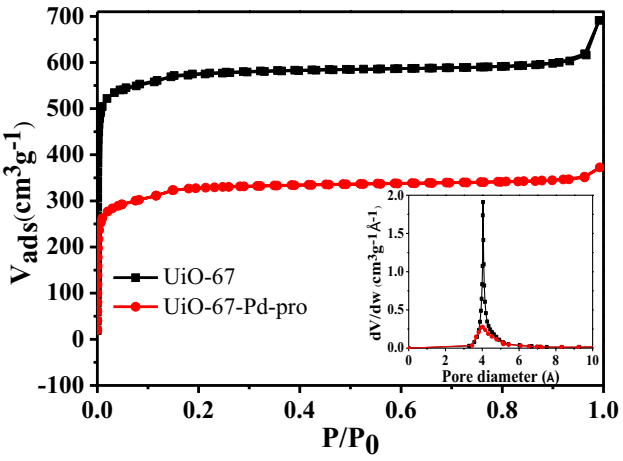

Fig. 2 N_2 adsorption–desorption isotherms of UiO-67 and UiO-67-Pd-pro

Pd(II)-metalated linker and 1,1'-biphenyl-4,4'-dicarboxylic acid was 1:1.4:2.75 (Fig. S2), suggesting the successful synthesis of multivariate UiO-67 via mixed-linker strategy.

The N_2 adsorption–desorption isotherms of UiO-67 and UiO-67-Pd-pro displayed typical Type I gas adsorption behaviour (Fig. 2). The BET specific surface area and pore volume of UiO-67-Pd-pro were, respectively, 1207.6 $m^2\ g^{-1}$ and 0.58 $cm^3\ g^{-1}$, lower than those of pure UiO-67 (2244.8 $m^2\ g^{-1}$ and 1.07 $cm^3\ g^{-1}$). Meanwhile, compared with the parent UiO-67, the pore size distribution of UiO-67-Pd-pro slightly decreased from 4.04 to 4.01 Å. These phenomena signified that the cavities of UiO-67-Pd-pro were partially blocked by large L-proline decorated and Pd(II)-metalated ligands [36].

In IR spectra of UiO-67-Pd-pro (Fig. S3), the peaks at 650 and 769 cm^{-1} can be ascribed to stretching vibration of Zr–O bonds [44]. Two strong peaks at 1260 and 1590 cm^{-1} corresponded to the characteristic of C–N and C=O bonds, respectively [95]. Moreover, the characteristic peak at 3400 cm^{-1} belonged to the vibration of N–H bond [96]. CD spectrum of UiO-67-Pd-pro was also measured, in which there was a negative Cotton effect at 222 nm and a positive cotton effect at 252 nm (Fig. S4), exhibiting the structural chirality of bulk samples [97–100].

X-ray photoelectron spectroscopy (XPS) spectra suggested the Pd element in UiO-67-Pd-pro was Pd^{2+} with two obvious peaks at 337.5 and 342.8 eV [101, 102], and no Pd^0 peaks were found (Fig. S5). Scanning electron microscopy (SEM) revealed that the as-prepared UiO-67-Pd-pro exhibited a uniform and regular octahedral morphology with

crystal size of 600–800 nm (Fig. S6). Transmission Electron Microscope (TEM) was further utilized to investigate the detailed structure information of the catalyst (Fig. 3). The results showed that no aggregated Pd particles were distinctly observed (Fig. 3a, b), which was in accordance with the conclusion of XPS. Moreover, in EDS mapping of UiO-67-Pd-pro, Cl, Pd and Zr displayed a consistent and even distribution (Fig. 3d–f), which further suggested the existence of Pd(II)-metalated ligands. Thermal stability of UiO-67-Pd-pro was tested via TGA and the sample remained intact till 280 °C (Fig. S7).

2.2 Sequential Suzuki Coupling/Asymmetric Aldol Reactions

The coexistence of Pd(II) and L-proline in UiO-67-Pd-pro made it have the potential in Suzuki Coupling/asymmetric Aldol sequential reactions as a bifunctional catalyst. The catalytic sequence can be divided into two steps: Suzuki Coupling (step I) and asymmetric Aldol reaction (step II). We then explored the optimal conditions of each step in sequence.

For Suzuki Coupling, the reaction of bromobenzene and 4-formylphenylboronic acid was selected as the template reaction to investigate the optimal catalytic conditions, such as base, temperature, reaction time and catalyst amount.

As shown in Table 1, we first studied the effect of inorganic base on the catalytic activity. Compared to Na_2CO_3, KF and CsF, K_2CO_3 was the best inorganic base (99%) (Table 1, entries 1–4). Thus, K_2CO_3 was used as the inorganic base. When the reaction temperature decreased from 90 to 50 °C, the yield was obviously reduced from 99 to 51% (Table 1, entries 2 and 5). Besides, the yield was only 45% and 87%, when the reaction was stopped after 8 and 12 h, respectively (Table 1, entries 6 and 7). The catalyst amount was reduced by half to 10 mg, and the yield was decreased to 82% (Table 1, entry 8). Comparison tests were performed, using UiO-67, UiO-67-pro or none as the catalyst (Table 1, entry 9–11), and there was no signs of conversion, suggesting that the metalated $PdCl_2$ in the MTV-MOF acted as the active sites.

Homogeneous $PdCl_2$ and $Pd(OAC)_2$, with the same amounts of Pd(II) sites, were employed as comparative catalysts, resulting in lower yields with 63% and 84%, respectively (Table 1, entries 12, 13), which may be attributed to the site-isolation of Pd^{2+} centers in UiO-67-Pd-pro and protection of MOF to avoid Pd^{2+} deactivation under air atmosphere [36].

As a result, UiO-67-Pd-pro exhibited outstanding catalytic yield of Suzuki coupling (99%) with K_2CO_3 as inorganic base at 90 °C for 16 h.

For asymmetric Aldol reaction, 4-phenylbenzaldehyde and cyclopentanone were selected as model substrates. The effect of solvent, catalyst amount and reaction temperature was investigated. Firstly, toluene, EtOH, CH_2Cl_2, DMSO and solvent-free, were employed as the reaction solvent, suggesting that DMSO was the optimal solvent with the higher yield and ee_{anti} value (Table 2, entries 1–5). When

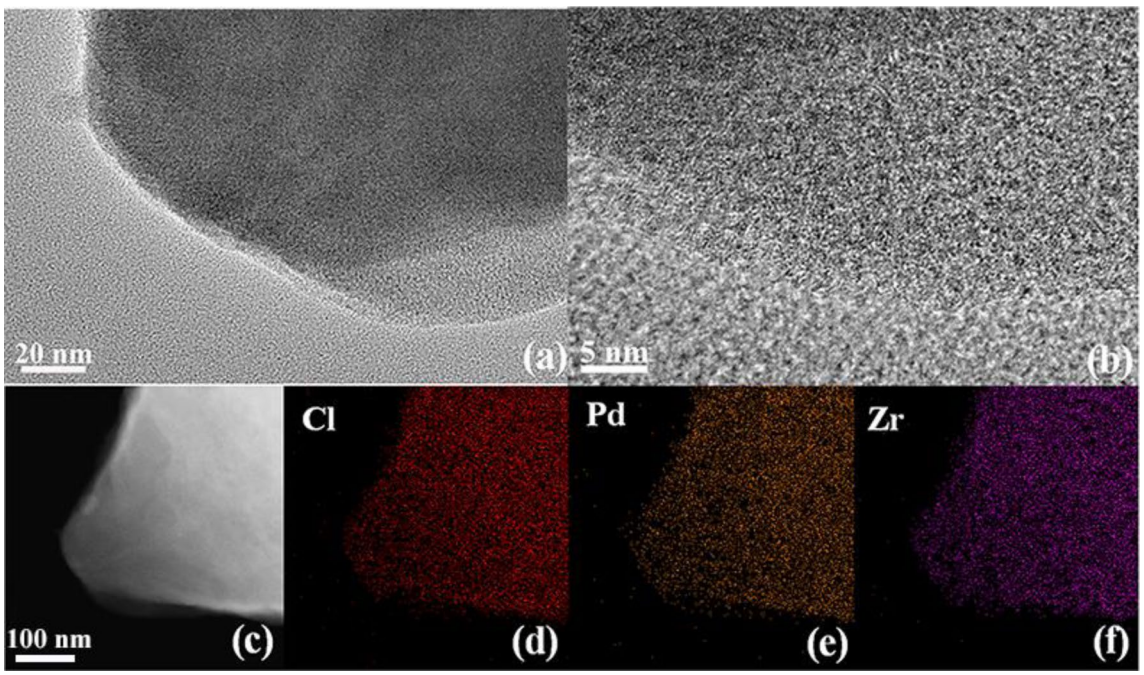

Fig. 3 **a**–**c** TEM images, **d** Cl, **e** Pd, **f** Zr distribution in EDX elemental mapping images of UiO-67-Pd-pro

Table 1 Exploration on reaction conditions of Suzuki cross-coupling reaction

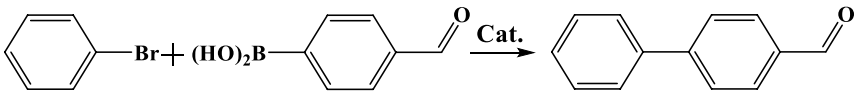

Entry	Catalyst	mg	Base	T (°C)	t (h)	Yield (%)[a]
1	UiO-67-Pd-pro	20	Na_2CO_3	90	16	85
2	UiO-67-Pd-pro	20	K_2CO_3	90	16	99
3	UiO-67-Pd-pro	20	KF	90	16	80
4	UiO-67-Pd-pro	20	CsF	90	16	59
5	UiO-67-Pd-pro	20	K_2CO_3	50	16	51
6	UiO-67-Pd-pro	20	K_2CO_3	90	8	45
7	UiO-67-Pd-pro	20	K_2CO_3	90	12	87
8	UiO-67-Pd-pro	10	K_2CO_3	90	16	82
9	UiO-67	20	K_2CO_3	90	16	n.d
10	UiO-67-pro	20	K_2CO_3	90	16	n.d
11[b]	none	0	K_2CO_3	90	16	n.d
12	$PdCl_2$	1.8	K_2CO_3	90	16	63
13	$Pd(OAc)_2$	2.2	K_2CO_3	90	16	84

Reaction conditions: 4-bromobenzaldehyde (1 mmol), phenylboronic acid (1.5 mmol), base (2 mmol), toluene (8 mL) and catalyst

[a]Isolate yield

[b]No catalyst

Table 2 Exploration on reaction conditions of asymmetric Aldol reaction

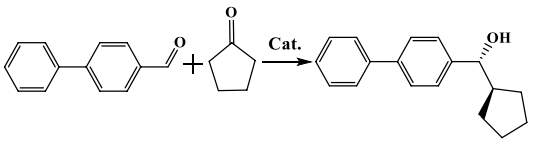

Entry	Catalyst	mg	Solvent	T (°C)	Yield (%)[a]	*syn*:*anti*[b]	ee_{anti} (%)[b]
1	UiO-67-Pd-pro	20	Toluene	20	67	52:48	1
2	UiO-67-Pd-pro	20	EtOH	20	75	68:32	1
3	UiO-67-Pd-pro	20	Free	20	59	55:45	4
4	UiO-67-Pd-pro	20	CH_2Cl_2	20	83	66:34	10
5	UiO-67-Pd-pro	20	DMSO	20	87	66:34	13
6	UiO-67-Pd-pro	10	DMSO	20	63	64:36	23
7	UiO-67-Pd-pro	20	DMSO	40	92	77:23	4
8	UiO-67-Pd-pro	20	CH_2Cl_2	-20	79	53:47	69
9	UiO-67	20	CH_2Cl_2	20	n.d	n.d	n.d
10	UiO-67-Pd	20	CH_2Cl_2	20	n.d	n.d	n.d

Reaction conditions: biphenyl-4-carbaldehyde (1 mmol), cyclopentanone (0.88 mL), solvent (2 mL), 4 days and catalyst

[a]Isolate yield

[b]Determined by chiral HPLC (chiral AD-H column, 1 mL min^{-1}, *n*-hexane: isopropanol = 90:10)

CH_2Cl_2 was utilized as the solvent, the yield and ee_{anti} value were slightly lower than those of DMSO (Table 2, entries 4, 5). Secondly, while the catalyst amount was reduced by half to 10 mg, the yield was only 63%, significantly lower than that of 20 mg catalyst (87%) (Table 2, entries 5 and 6). Finally, considering the important influence of temperature on diastereoselectivity and enantioselectivity of asymmetric catalysis, the reaction was performed at 40 °C. The yield was increased to 92%, but the ee_{anti} value was only 4% (Table 2, entry 7). Thus, we tried to low the temperature. Because of high freezing point of DMSO (18.4 °C), CH_2Cl_2 with the second best catalytic performances was selected as the solvent at -20 °C, resulting in slightly lower yield (79%) but greatly improved ee_{anti} value (69%). Therefore, CH_2Cl_2, − 20 °C, 20 mg catalyst were chosen as the optimal conditions for the asymmetric Aldol condensation reaction.

As UiO-67 and UiO-67-Pd were, respectively, used to replace UiO-67-Pd-pro as the catalyst, there was no product observed (Table 2, entries 9, 10), indicating that L-proline in the MTV-MOF acted as the catalytic sites of asymmetric Aldol reactions.

Remarkably, compared with other L-proline functionalized MOFs, UiO-67-Pd-pro exhibited superior performances for catalyzing asymmetric Aldol reactions (Table S1).

After the optimal conditions of Suzuki Coupling (step I) and asymmetric Aldol reaction (step II) were confirmed, the model sequential reaction was further performed. Considering the negative effect of inorganic base (K_2CO_3) and solvent (toluene) in step I, on the performance of step II, the residual K_2CO_3 was neutralized with diluted HCl and the solvent was also removed via rotary vacuum evaporation after the coupling was over.

The optimal conditions were finally popularized to other substituted substrates for asymmetrical sequential reactions (Table 3). It can be easily seen that regardless of the substituents, UiO-67-Pd-pro showed excellent catalytic activity (94–99%) in the Suzuki coupling reaction. Although the yield of Aldol reaction was moderate, the catalyst exhibited satisfied enantioselectivities with ee_{anti} values up to 98%.

2.3 Heterogeneous and Recycling Experiments

In order to verify the heterogeneous nature of the catalyst, two experiments were performed. First, after the model sequential reaction was finished, the supernatant was measured via ICP-OES and the results showed that only Zr and Pd traces (< 0.20 ppm) were found, hinting that there was

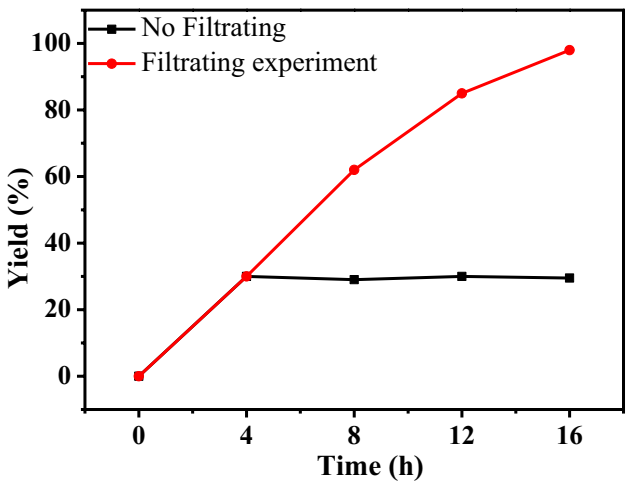

Fig. 4 Hot leaching test of Suzuki coupling reaction

Table 3 Substrate exploration of sequential Suzuki coupling/asymmetric Aldol reactions

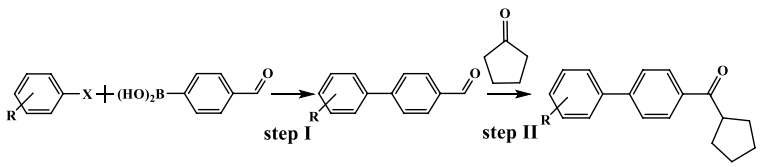

Entry	R	X	RCHO yield[a] (%)	Aldol Yield[a] (%)	syn:anti[b]	ee_{anti}[b] (%)
1	H	Br	99	79	56:44	68
2	4-CH_3	I	96	65	89:11	75
3	4-CH_3O	I	94	69	83:17	86
4	4-CN	I	98	83	50:50	56
5	4-NO_2	Br	99	88	2:98	98

[a]Isolate yield

[b]Determined by chiral HPLC (chiral AD-H column, 1 mL min^{-1}, *n*-hexane: isopropanol = 90:10)

almost no leaching of Zr and Pd elements from UiO-67-Pd-pro during the catalysis process. Second, a hot leaching test was investigated (Fig. 4). After the model Suzuki coupling reaction was carried out for 4 h, the solid catalyst was separated by hot filtration, and then the reaction was continued. It was found that the yield of coupling reaction did not increase with the increase of reaction time, while the reaction continued to proceed when the catalyst wasn't separated from the system.

In order to find out whether the reaction occurred on the surfaces or inside the pores of the catalyst, macrosubstrate experiments were performed (Table S2). A bulk aldehyde with the size of 9 Å × 14 Å, far larger than the pore size of UiO-67-Pd-pro (4 Å), was used to Aldol reaction. No corresponding microaldol product was observed via HPLC test after 2 weeks of reaction, while the aldol product achieved 51% yield for 48 h by the use of the homogeneous catalyst, L-proline. This result suggested that the reaction took place inside the pores with the use of UiO-67-Pd as the catalyst.

Recycling experiments showed that the catalytic activity and enantioselectivity of the catalyst did not have a significant decrease within three catalytic cycles (Fig. 5). Moreover, the catalyst maintained structural stability after three cycles, measured via XRD (Fig. 1a). Thus, the UiO-67-Pd-pro catalyst had excellent cycle stability.

2.4 Comparison of Catalytic Performance Between UiO-67-Pd-pro and Pd@NH_2-UiO-66(pro)-1

In order to prove that Pd^{2+} in synthetic catalyst UiO-67-Pd-pro has better catalytic performance in Suzuki cross-coupling reaction, we compared it with the previously reported elemental Pd catalyst Pd@NH_2-UiO-66(pro)-1 [44]. As shown in Fig. 6,

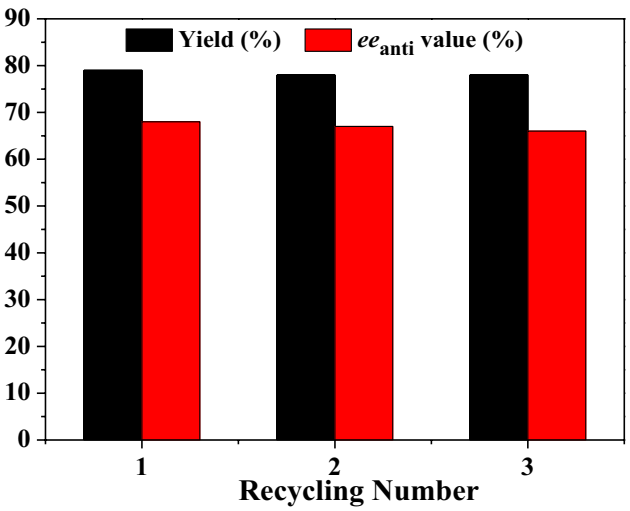

Fig. 5 Recycling experiments of UiO-67-Pd-pro about sequential Suzuki Coupling/asymmetric Aldol reactions

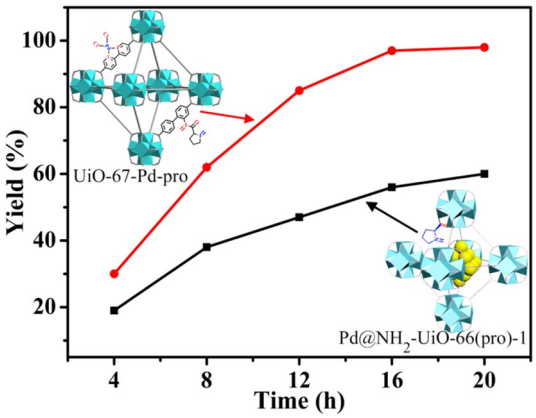

Fig. 6 Compare the catalytic performances of two different Pd catalysts

it can be clearly observed that the catalytic performance of UiO-67-Pd-pro was obviously superior to that of Pd@NH_2-UiO-66(pro)-1 when the reaction time reached 16 h. With the increase of time, the catalytic performance of UiO-67-Pd-pro was in equilibrium, which was mainly attributed to the high utilization rate of UiO-67-Pd-pro for Pd ion coordination. Pd@NH_2-UiO-66(pro)-1 has a slight increase, mainly due to Pd nanoparticles aggregation resulting in less active sites exposure.

3 Conclusions

In summary, we have successfully designed and fabricated a Pd(II)-metalated and L-proline-decorated chiral MTV-MOF via mixed-linker strategy. The combination of Pd(II) and L-proline bifunctional active sites promoted the MOF to be an effective heterogeneous catalyst for Suzuki Coupling/asymmetric Aldol sequential reactions. The catalyst exhibited remarkably higher performance than its homogeneous counterpart, $PdCl_2$. ICP-OES measurements of the supernatant and hot leaching test showed the heterogeneous nature of the catalyst. Macrosubstrate tests also verified that the reaction occurred inside the pores of the MOF. The catalyst can be recycled for 3 times without obvious structural change and loss of catalytic activity. This work may provide a simple but efficient strategy to design multifunctional MTV-MOF catalysts for sequential/tandem reactions via mixed-linker strategy.

4 Experimental

4.1 Materials

4-Methoxyphenylboronic acid, $Pd(PPh_3)_4$, N-Boc-L-proline, 2,2'-bipyridine-5,5'-dicarboxylic acid, $ZrCl_4$,

$PdCl_2(CH_3CN)_2$, ethyl 4-bromo-3-aminobenzoate and 2,2'-biphenyl-5,5'-dicarboxylic acid (H_2bpdc) were obtained from Sinopharm Chemical Reagent Co. Ltd. Catalytic substrates were bought from Aladdin. Isopropyl alcohol and *n*-hexane for HPLC were acquired from Tedia and Merck, respectively. All the reagents were directly used as received without further purification.

4.2 Synthesis of the Ligands

L-proline decorated ligand, *R*-2-(pyrrolidine-2-carboxamido)-[1,1'-biphenyl]-4,4'-dicarboxylic acid [79], and Pd(II)-metalated ligand, Pd(2,2'-bipyridine-5,5'-dicarboxylic acid)Cl_2 [75], were synthesized according to the similar procedures previously reported and the detailed processes were shown in supporting information.

4.3 Synthesis of the MOFs

4.3.1 Synthesis of UiO-67

$ZrCl_4$ (24.5 mg, 0.105 mmol), H_2bpdc (25.4 mg, 0.105 mmol) were added in 4 mL DMF. The mixture was evenly dispersed by sonication for about 10 min, then transferred to a reaction kettle and kept at 100 °C for 36 h. The solid was collected by centrifugation and washed with DMF (3 × 10 mL) and methanol (3 × 10 mL). Before catalyzed the Suzuki/Aaymmetric Aldol sequential reaction, the synthesized catalyst was immersed in 10 mL methanol solution for 3 days. Fresh solvent was replaced for 24 h, and then the activated catalyst was dried via vacuum.

4.3.2 Synthesis of UiO-67-pro

$ZrCl_4$ (24.5 mg, 0.105 mmol), H_2bpdc (19.1 mg, 0.079 mmol) and chiral L-proline decorated ligand (9.3 mg, 0.026 mmol) were added in 4 mL DMF. The subsequent steps of reaction and washing were the same as the preparation of UiO-67.

4.3.3 Synthesis of UiO-67-Pd

$ZrCl_4$ (24.5 mg, 0.105 mmol), H_2bpdc (19.1 mg, 0.079 mmol) and Pd(II)-metalated ligand (11.1 mg, 0.026 mmol) were added in 4 mL DMF. The subsequent steps of reaction and washing were the same as the preparation of UiO-67.

4.3.4 Synthesis of UiO-67-Pd-pro

$ZrCl_4$ (24.5 mg, 0.105 mmol), H_2bpdc (12.7 mg, 0.052 mmol), chiral L-proline decorated ligand (9.3 mg, 0.026 mmol) and Pd(II)-metalated ligand (11.1 mg, 0.026 mmol) were added in 4 mL DMF. The subsequent steps of reaction and washing were the same as the preparation of UiO-67.

4.4 General Catalytic Procedures

4.4.1 General Procedure for Suzuki Coupling Reaction Catalyzed by UiO-67-Pd-pro

In a round-bottom flask, aryl halide (1 mmol), 4-formylphenylboronic acid (225 mg, 1.5 mmol), UiO-67-Pd-pro (20 mg), and K_2CO_3 (276 mg, 2 mmol) were added into toluene (8 mL). The reaction mixture was stirred in air atmosphere at 90 °C for 16 h. The reaction products were monitored by TLC to determine whether the substrate was completely consumed. After centrifugation, the solvent was removed by rotary evaporation and purification by chromatography column, giving a white solid product.

4.4.2 General Procedure for Asymmetric Aldol Reaction Catalyzed by UiO-67-Pd-pro

A mixture of biphenyl formaldehyde (1 mmol), cyclopentanone (0.88 mL, 10 mmol), dichloromethane (2 mL) and the catalyst UiO-67-Pd-pro (20 mg) was stirred at the certain temperature in Table 2 for 5 days. The solid catalyst was removed by filtration and the organic phase was concentrated in vacuo, and purified by flash column chromatography. The *ee* value and *dr* value of the product were calculated by HPLC spectra (chiral column AD-H, n-hexane: isopropanol = 90:10, flow rate: 1 mL min^{-1}).

4.4.3 General Procedure for Suzuki/Asymmetric Aldol Sequential Reactions Catalyzed by UiO-67-Pd-pro

In a toluene (8 mL) solution, aryl halide (1 mmol), 4-formylphenylboronic acid (225 mg, 1.5 mmol), UiO-67-Pd-pro (20 mg), and K_2CO_3 (276 mg, 2 mmol) were reacted under specific conditions. After the coupling procedure was completed, the reaction mixture was cooled to room temperature. Considering the influence of K_2CO_3 and toluene on asymmetric aldol reactions, after the coupling procedure was completed, the reaction mixture was cooled to room temperature and then neutralized with 1 M HCl. The solvent was also evaporated under reduced pressure. Cyclopentanone (0.88 mL, 10 mmol) and CH_2Cl_2 (2 mL) were added into the above residue, followed by applied ultrasonic treatment for 10 min. Then the mixture was stirred at − 20 °C. The product was collected by fast column chromatography and analyzed by HPLC spectra (chiral AD-H column, *n*-hexane: isopropanol = 90: 10, 1 mL min^{-1}).

Supplementary Information The online version contains supplementary material available at https://doi.org/10.1007/s10562-021-03719-0.

Acknowledgements This work was supported by the Priority Academic Program Development of Jiangsu Higher Education Institutions, National Natural Science Foundation of China (No. 21471031) and Fundamental Research Funds for the Central Universities.

Declarations

Conflict of interest The authors declare that there is no conflict of interests regarding the publication of this paper.

References

1. Wasilke JC, Obrey SJ, Baker RT, Bazan GC (2005) Chem Rev 105:1001–1020
2. Thomas CM (2012) Chem Soc Rev 41:7712–7722
3. Wu PY, He C, Wang J, Peng XJ, Li XZ, An YL, Duan CY (2012) J Am Chem Soc 134:14991–14999
4. Park J, Li JR, Chen YP, Yu JM, Yakovenko AA, Wang ZYU, Sun LB, Balbuena PB, Zhou HC (2012) Chem Commun 48:9995–9997
5. Srirambalaji R, Hong S, Natarajan R, Yoon M, Hota R, Kim Y, Ko YH, Kim K (2012) Chem Commun 48:11650–11652
6. He HM, Sun FX, Aguila B, Perman JA, Ma SQ, Zhu GS (2016) J Mater Chem A 4:15240–15246
7. Zhao SY, Chen ZY, Wei N, Liu L, Han ZB (2019) Inorg Chem 58:7657–7661
8. Sheng K, Fan LM, Tian XF, Gupta RK, Gao LN, Tung CH, Sun D (2020) Sci Chin Chem 63:182–186
9. Dau PV, Cohen SM (2015) Inorg Chem 54:3134–3138
10. Shaabani A, Mohammadian R, Hashemzadeh A, Afshari R, Amini MM (2018) New J Chem 42:4167–4174
11. Chung YM (2018) Res Chem Intermed 44:3673–3685
12. Zhang Y, Wang YX, Liu L, Wei N, Gao N, Zhao D, Han ZB (2018) Inorg Chem 57:2193–2198
13. Mistry S, Sarkar A, Natarajan S (2019) Cryst Growth Des 19:747–755
14. Ma LQ, Abney C, Lin WB (2009) Chem Soc Rev 38:1248–1256
15. Jiao L, Wang Y, Jiang HL, Xu Q (2018) Adv Mater 30:1703663
16. Zhang WX, Liao PQ, Lin RB, Wei YS, Zeng MH, Chen XM (2015) Coord Chem Rev 293:263–278
17. Huang YB, Liang J, Wang XS, Cao R (2017) Chem Soc Re 46:126–157
18. Berijani K, Morsali A (2021) Inorg Chem 60:206–218
19. Karmakar A, Pombeiro AJL (2019) Coord Chem Rev 395:86–129
20. Cheng L, Yang JH, Zhai QC, Zhang QS (2020) Chin J Inorg Chem 36:361–367
21. Yin Z, Wan S, Yang J, Kurmoo M, Zeng MH (2019) Coord Chem Rev 378:500–512
22. Mutiah M, Sebastien R, Ida A, Andrew DB, Emma ACM (2021) Chem Eng Process 161:108315
23. Lirio S, Shih YH, So PB, Liu LH, Yen YT, Furukawa S, Liu WL, Huang HY, Lin CH (2021) Dalton Trans 50:1866–1873
24. Corma A, Garcia H, Xamena FXLI (2010) Chem Rev 110:4606–4655
25. Yoon M, Srirambalaji R, Kim K (2012) Chem Rev 112:1196–1231
26. Liu JW, Chen LF, Cui H, Zhang JY, Zhang L, Su CY (2014) Chem Soc Rev 43:6011–6061
27. Chughtai AH, Ahmad N, Younus HA, Laypkov A, Verpoort F (2015) Chem Soc Rev 44:6804–6849
28. Song Y, Feng XY, Chen JS, Brzezinski C, Xu ZW, Lin WB (2020) J Am Chem Soc 142:4872–4882
29. Zeng LZ, Wang ZY, Wang YK, Wang J, Guo Y, Hu HH, He XF, Wang C, Lin WB (2020) J Am Chem Soc 142:75–79
30. Kobayashi A, Ohba T, Saitoh E, Suzuki Y, Noro S, Chang HC, Kato M (2014) Inorg Chem 53:2910–2921
31. Kim D, Whang DR, Park SY (2016) J Am Chem Soc 138:8698–8701
32. Miera GG, Gómez AB, Chupas PJ, Martín-Matute B, Chapman KW, Platero-Prats AE (2017) Inorg Chem 56:4576–4583
33. Marshall RJ, Lennon CT, Tao A, Senn HM, Wilson C, Fairen-Jimenez D, Forgan RS (2018) J Mater Chem A 6:1181–1187
34. Wang XN, Zhang P, Kirchon A, Li JL, Chen WM, Zhao YM, Li B, Zhou HC (2019) J Am Chem Soc 141:13654–13663
35. Wang C, Lin WB (2011) J Am Chem Soc 133:4232–4235
36. Manna K, Zhang T, Lin WB (2014) J Am Chem Soc 136:6566–6569
37. Zhang T, Manna K, Lin WB (2016) J Am Chem Soc 138:3241–3249
38. An B, Zhang JZ, Cheng K, Ji PF, Wang C, Lin WB (2017) J Am Chem Soc 139:3834–3840
39. Xu RY, Drake T, Lan GX, Lin WB (2018) Chem Eur J 24:15772–15776
40. Song FJ, Wang C, Lin WB (2011) Chem Commun 47:8256–8258
41. Han QX, Qi B, Ren WM, He C, Niu JY, Duan CY (2015) Nat Commun 6:10007
42. Li ZJ, Liu Y, Kang X, Cui Y (2018) Inorg Chem 57:9786–9789
43. Gong W, Chen X, Jiang H, Chu DD, Cui Y, Liu Y (2019) J Am Chem Soc 141:7498–7508
44. Cheng L, Zhao KY, Zhang QS, Li YM, Zhai QC, Chen JX, Lou YB (2020) Inorg Chem 59:7991–8001
45. Li ZJ, Liu Y, Xia QC, Cui Y (2017) Chem Commun 53:12313–12316
46. Xia QC, Li ZJ, Tan CX, Liu Y, Gong W, Cui Y (2017) J Am Chem Soc 139:8259–8266
47. Jiao JJ, Tan CX, Li ZJ, Liu Y, Han X, Cui Y (2018) J Am Chem Soc 140:2251–2259
48. Xia QC, Yuan C, Li YX, Cui Y (2019) Chem Commun 55:9136–9139
49. Deng HX, Doonan CJ, Furukawa H, Ferreira RB, Towne J, Knobler CB, Wang B, Yaghi OM (2010) Science 327:846–850
50. Dhakshinamoorthy A, Asiri AM, Garcia H (2016) Catal Sci Technol 6:5238–5261
51. Helal A, Yamani ZH, Cordova KE, Yaghi OM (2017) Natl Sci Rev 4:296–298
52. Bitzer J, Kleist W (2019) Chem Eur J 25:1866–1882
53. Feng L, Wang KY, Daya GS, Zhou HC (2019) Chem Soc Rev 48:4823–4853
54. Jiao JJ, Gong W, Wu XW, Yang SP, Cui Y (2019) Coord Chem Rev 385:174–190
55. Kong XQ, Deng HX, Yan FY, Kim JH, Swisher JA, Smit B, Yaghi OM, Reimer JA (2013) Science 341:882–885
56. Li HN, Yang Y, He C, Zeng L, Duan CY (2019) ACS Catal 9:422–430
57. Sun YJ, Sun LX, Feng DW, Zhou HC (2016) Angew Chem Int Ed 55:6471–6475
58. Lia TT, Liu YM, Wang T, Wu YL, He YL, Yang R, Zheng SR (2018) Microporous Mesoporous Mater 272:101–108
59. Fang ZL, Durholt JP, Kauer M, Zhang WH, Lochenie C, Jee B, Albada B, Metzler-Nolte N, Poppl A, Weber B, Muhler M, Wang YM, Schmid R, Fischer RA (2014) J Am Chem Soc 136:9627–9636
60. Yuan S, Lu WG, Chen YP, Zhang Q, Liu TF, Feng DW, Wang X, Qin JS, Zhou HC (2015) J Am Chem Soc 137:3177–3180
61. Liu Q, Cong HJ, Deng HX (2016) J Am Chem Soc 138:13822–13825

62. Dong ZY, Sun YZS, Chu J, Zhang XZ, Deng HX (2017) J Am Chem Soc 139:14209–14216
63. Liang J, Xie YQ, Wu Q, Wang XY, Liu TT, Li HF, Huang YB (2018) Inorg Chem 57:2584–2593
64. He L, Natha JK, Lin QP (2019) Chem Commun 55:412–415
65. Ma RQ, Jiang HQ, Wang C, Zhao CB, Deng HX (2020) Chem Commun 56:2715–2718
66. Feng L, Yuan S, Zhang LL, Tan K, Li JL, Kirchon A, Liu LM, Zhang P, Han Y, Chabal YJ, Zhou HC (2018) J Am Chem Soc 140:2363–2372
67. Pang JD, Yuan S, Qin JS, Wu MY, Lollar CT, Li JL, Huang N, Li B, Zhang P (2018) J Am Chem Soc 140:12328–12332
68. Cao CC, Chen CX, Wei ZW, Qiu QF, Zhu NX, Xiong YY, Jiang JJ, Wang DW, Su CY (2019) J Am Chem Soc 141:2589–2593
69. Mon M, Bruno R, Tiburcio E, Viciano-Chumillas M, Kalinke LHG, Ferrando-Soria J, Armentano D, Pardo E (2019) J Am Chem Soc 141:13601–13609
70. Liu LZ, Yao ZZ, Ye YX, Yang YK, Lin QJ, Zhang ZJ, O'Keeffffe M, Xiang SC (2020) J Am Chem Soc 142:9258–9266
71. Fan WD, Yuan S, Wang WJ, Feng L, Liu XP, Zhang XR, Wang X, Kang ZX, Dai FN, Yuan DQ, Sun DF, Zhou HC (2020) J Am Chem Soc 142:8728–8737
72. Jrad A, Hmadeh M, Awada G, Chakleh R, Ahmad M (2021) Chem Eng J 410:128237
73. Razan L, Fayrouz AI, Mazen AG, Mohamad H (2021) Nano Res 14:423–431
74. Wang Y, Lv H, Grape ES, Gaggioli CA, Tayal A (2021) J Am Chem Soc 143:6333–6338
75. Beyzavi MH, Vermeulen NA, Zhang KN, So M, Kung CW, Hupp JT, Farha OK (2016) ChemPlusChem 81:708–713
76. Huang SL, Jia AQ, Jin GX (2013) Chem Commun 49:2403–2405
77. Chen LY, Rangan S, Li J, Jiang HF, Li YW (2014) Green Chem 16:3978–3985
78. Bloch ED, Britt D, Lee C, Doonan CJ, Uribe-Romo FJ, Furukawa H, Long JR, Yaghi OM (2010) J Am Chem Soc 132:14382–14384
79. Fei HH, Cohen SM (2014) Chem Commun 50:4810–4812
80. Jia SP, Xiao X, Li QY, Li Y, Duan ZG, Li YY, Li XT, Lin ZH, Zhao YG, Huang W (2019) Inorg Chem 58:12748–12755
81. Banerjee M, Das S, Yoon M, Choi HJ, Hyun MH, Park SM, Seo G, Kim K (2009) J Am Chem Soc 131:7524–7525
82. Rossini AJ, Zagdoun A, Lelli M, Canivet J, Aguado S, Ouari O, Tordo P, Rosay M, Maas WE, Copéret C, Farrusseng D, Emsley L, Lesage A (2012) Angew Chem Int Ed 51:123–127
83. Kutzscher C, Hoffmann HC, Krause S, Stoeck U, Senkovska I, Brunner E, Kaskel S (2015) Inorg Chem 54:1003–1009
84. Kutzscher C, Nickerl G, Senkovska I, Bon V, Kaskel S (2016) Chem Mater 28:2573–2580
85. Fracaroli AM, Siman P, Nagib DA, Suzuki M, Furukawa H, Toste FD, Yaghi OM (2016) J Am Chem Soc 138:8352–8355
86. Marshall RJ, Hobday CL, Murphie CF, Griffin SL, Morrison CA, Moggach SA, Forgan RS (2016) J Mater Chem A 4:6955–6963
87. Gutov OV, Molina S, Escudero-Adán EC, Shafir A (2016) Chem Eur J 22:13582–13587
88. Liu J, Zhou TY, Telfer SG (2017) J Am Chem Soc 139:13936–13943
89. Nguyen KD, Kutzscher C, Drache F, Senkovska I, Kaskel S (2018) Inorg Chem 57:1483–1489
90. Todorova TK, Rozanska X, Gervais C, Legrand A, Ho LN, Berruyer P, Lesage A, Emsley L, Farrusseng D, Canivet J, Mellot-Draznieks C (2016) Chem Eur J 22:16531–16538
91. Wang PP, Chen DP, Wang SH, Chen C (2017) Chin J Inorg Chem 33:817–822
92. Feng X, Jena HS, Leus K, Wang GB, Ouwehand J, Van Der Voort P (2018) J Catal 365:36–42
93. Dong XW, Yang Y, Che JX, Zuo J, Li XH, Gao L, Hua YZ, Liu XY (2018) Green Chem 20:4085–4093
94. Dzesse TCN, Nfor EN, Bourne SA (2018) Cryst Growth Des 18:416–423
95. Nguyen KD, Kutzscher C, Ehrling S, Senkovska I, Bon V, de Oliveira JM, Gutmann T, Buntkowsky G, Kaskel S (2019) J Catal 377:41–50
96. Niessing S, Janiak C (2019) Mol Catal 467:70–77
97. Gascon J, Aktay U, Hernandez-Alonso MD, van Klink GPM, Kapteijn F (2009) J Catal 261:75–87
98. Pan XB, Xu HT, Zhao X, Zhang HQ (2020) ACS Sustain Chem Eng 8:1087–1094
99. Cheng L, Wang J, Qi Q, Zhang XY, Yu HY, Gou SH, Fang L (2014) CrystEngComm 16:10056–10065
100. Ren H, Cheng L, Yang JH, Zhao KY, Zhai QC, Li YM (2021) Catal Commun 149:106249
101. Tiburcio E, Greco R, Mon M, Ballesteros-Soberanas J, Ferrando-Soria J, López-Haro M, Hernandez-Garrido JC, Oliver-Meseguer J, Marini C, Boronat M, Armentano D, Leyva-Pérez A, Pardo E (2021) J Am Chem Soc 143:2581–2592
102. Fortea-Pérez FR, Mon M, Ferrando-Soria J, Boronat M, Leyva-Pérez A, Corma A, Herrera JM, Osadchii D, Gascon J, Armentano D, Pardo E (2017) Nat Mater 16:760–766